inorganics

MDPI

Article

$Ni(NH_3)_2(NO_3)_2$—A 3-D Network through Bridging Nitrate Units Isolated from the Thermal Decomposition of Nickel Hexammine Dinitrate

Joachim Breternitz [1,2], Agata Godula-Jopek [3,4] and Duncan H. Gregory [1,*]

1 WestCHEM School of Chemistry, University of Glasgow, University Avenue, Glasgow G12 8QQ, UK
2 Helmholtz-Zentrum Berlin für Materialien und Energie, Department Structure and Dynamics of Energy Materials, Hahn-Meitner-Platz 1, 14109 Berlin, Germany; joachim.breternitz@helmholtz-berlin.de
3 Airbus Group Innovations, XCXDI, 81663 Munich, Germany; agata.godula-jopek@airbus.com
4 Institute of Chemical Engineering, Polish Academy of Sciences, 44100 Gliwice, Poland
* Correspondence: Duncan.Gregory@glasgow.ac.uk; Tel.: +44-141-330-8128

Received: 14 May 2018; Accepted: 1 June 2018; Published: 5 June 2018

Abstract: Nickel nitrate diammine, $Ni(NH_3)_2(NO_3)_2$, can be synthesised from the thermal decomposition of nickel nitrate hexammine, $Ni[(NH_3)_6](NO_3)_2$. The hexammine decomposes in two distinct major stages; the first releases 4 equivalents of ammonia while the second involves the release of NO_x, N_2, and H_2O to yield NiO. The intermediate diammine compound can be isolated following the first deammoniation step or synthesised as a single phase from the hexammine under vacuum. Powder X-ray diffraction (PXD) experiments have allowed the structure of $Ni(NH_3)_2(NO_3)_2$ to be solved for the first time. The compound crystallises in orthorhombic space group $Pca2_1$ (a = 11.0628 (5) Å, b = 6.0454 (3) Å, c = 9.3526 (4) Å; Z = 4) and contains 11 non-hydrogen atoms in the asymmetric unit. Fourier transform infrared (FTIR) spectroscopy demonstrates that the bonding in the ammine is consistent with the structure determined by PXD.

Keywords: crystal structure; ammine complex; structure determination; ammonia storage; vibrational spectroscopy

1. Introduction

Ammonia is increasingly being considered as a safe, readily available alternative to hydrogen as an energy vector with an energy density of 13.6 $GJ \cdot m^{-3}$ (at 10 bar) [1] and the added advantage of possible storage at high gravimetric and volumetric capacities. Ammonia itself contains 17.6 wt % hydrogen and could be employed as a hydrogen carrier, releasing hydrogen via catalytic cracking.

Metal ammine salts are attracting considerable interest as potential ammonia storage materials [2]. Transition metal salts readily form ammoniate complexes (ammines) with variable and controllable ammonia content [3]. The highest capacity (gravimetric density of ammonia) materials—typically hexammines—can be synthesised simply by the ambient temperature and pressure ammoniation of the respective transition metal salts. In an earlier study, we identified nickel salts as a promising group of ammonia storage materials [4]. Associated with this work, we were able to demonstrate that the reaction of ammonia with nickel nitrate hexahydrate induces ligand exchange and the growth of nickel nitrate hexammine crystals [5]. The thermal decomposition of nickel nitrate hexammine has been discussed previously in the literature [6,7] and the products of the decomposition tentatively identified. The structure of the proposed thermodynamically stable intermediate decomposition product nickel diammine nitrate has remained unknown. In this work, we revisit the thermal decomposition of $[Ni(NH_3)_6](NO_3)_2$ and determine the conditions for synthesis of the respective

diammine $Ni(NH_3)_2(NO_3)_2$. The successful preparation of the compound as a single phase has allowed us to determine its crystal structure for the first time and to perform a vibrational spectroscopy analysis of its bonding.

2. Results and Discussion

2.1. Thermal Decomposition of $[Ni(NH_3)_6](NO_3)_2$

Nickel hexammine, $[Ni(NH_3)_6](NO_3)_2$, was prepared using our previously published method, and its complete characterisation is discussed therein [5]. $[Ni(NH_3)_6](NO_3)_2$ was studied by simultaneous thermal analysis that combined thermogravimetry (TG), differential thermal analysis (DTA), and evolved gas analysis by mass spectrometry (MS) in the same experiment (Figure 1). The thermal decomposition of the material is evidently complex and clear steps are, especially at higher temperatures, hard to distinguish. Considering the evolved gas mass spectra (Figure 1b), the initial decomposition that occurs below approximately 200 °C can be attributed exclusively to the loss of ammonia, but not all the ammonia ligands are apparently removed before further decomposition products (from the decomposition of the nitrate anion) are detected. Therefore, the continued mass loss from the sample in the region of 200–300 °C must be interpreted in terms of simultaneous loss of further ammonia from the ammine complex in addition to nitrogen and nitrous oxides from the nitrate anions. From the identity of the evolved gases in the mass spectra, there is evidently a reaction between fragments from the ammonia ligands and the nitrate anion. It is interesting that no ammonia evolution is detected at temperatures above 300 °C, where N_2, N_2O, NO, and H_2O prevail. Ultimately only H_2O is released at high temperatures. These observed gaseous products match well to those observed previously for the decomposition of the hexammine nitrate in either argon or helium [6,7].

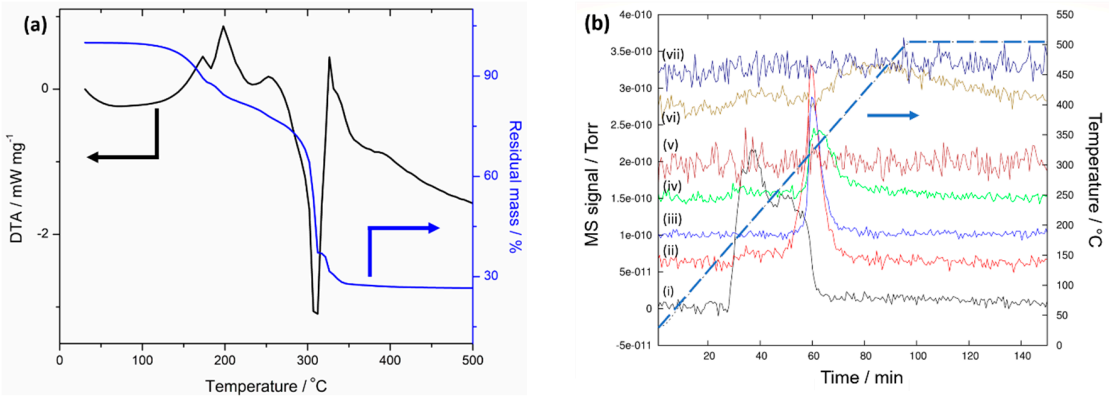

Figure 1. (**a**) Simultaneous thermal analysis of $[Ni(NH_3)_6](NO_3)_2$ showing the thermogravimetric (TG; blue) and differential thermal analysis (DTA; black) profiles. (**b**) Evolved gas analysis by mass spectrometry (MS) for (i) m/z = 17 (NH_3^+, black), (ii) m/z = 28 (N_2^+, red), (iii) m/z = 44 (N_2O^+, blue), (iv) m/z = 30 (NO^+, green), (v) m/z = 46 (NO_2^+, brown),(vi) m/z = 18 (H_2O^+, olive), and (vii) m/z = 2 (H_2^+, navy). The baselines are displaced along the *y*-axis for better visibility. The corresponding temperature is given by the dotted line.

It could be concluded that $[Ni(NH_3)_6](NO_3)_2$ firstly loses ammonia to form lower ammine complexes, before loss of the remaining ammonia molecules coincides with the decomposition of the nitrate anions into nitrogen and nitrous oxides. This would leave a solid product of nickel hydroxide, $Ni(OH)_2$, which itself further decomposes into nickel oxide with the loss of water (in the final step). The first decomposition mass loss (Table 1) of 11.8% corresponds well to the theoretical mass loss for the formation of the hypothetical tetrammine nickel nitrate, $[Ni(NH_3)_4](NO_3)_2$ (11.94%). The immediate subsequent mass loss, however, is not itself large enough to account for the formation of either the triammine or diammine nickel nitrate (theoretically 17.91% and 23.88%, respectively). In fact,

the three successive endotherms observed in the DTA trace below 300 °C would suggest that 2, 1, and 1 equivalents of ammonia are lost, resulting in the formation of the diammine, and the weight loss by the end of the third endotherm (of ca. 23 wt %) corresponds well to this assumption, even though the mass is not constant at this point. There is thus no clear endpoint after the ammonia release, and the sharp change in slope of the mass loss likely originates from the immediate onset of nitrate anion decomposition close to 300 °C. Steps 4 and 5 (Table 1) lie rather close to the expected mass losses for the formation of $Ni(OH)_2$ (67.44%) and NiO (73.77%) and hence underline the decomposition of the nitrate anion at higher temperatures. Given these results (most notably the DTA and MS data), we decided to use 200 °C as the lowest possible temperature for the formation of the diammine nickel nitrate while avoiding the decomposition of the nitrate anions. To drive the ammonia desorption, we performed the thermal treatment under mild dynamic vacuum to facilitate the removal of ammonia from the system.

Table 1. TG–DTA–MS analysis results for $[Ni(NH_3)_6](NO_3)_2$.

Step	Cumulative Mass Change/%	TG Temperatures/°C		DTA Peak Temperatures/°C	Gases Evolved (from MS)
		Onset	Final		
1	−11.8	107	179	173	NH_3
2	−16.9	187	208	198	NH_3
3	−23.4	208	262	257	NH_3
4	−63.1	272	316	309	NH_3, N_2, N_2O, NO
5	−72.7	321	375	336	H_2O

2.2. Crystal Structure Solution of $Ni(NH_3)_2(NO_3)_2$

When assessing the powder X-ray diffraction pattern of the thermal decomposition product, it showed sharp reflections but bore no similarities to previously described crystal structures in the system. Attempts to automatically index the pattern using the programs Ito [8], Treor [9], Dicvol [10], and McMaille [11] were successful and yielded consistent results, giving an orthorhombic cell with $a \approx 11.1$ Å, $b \approx 6.0$ Å, and $c \approx 9.4$ Å. In our experience, the use of more than one indexing program greatly increases the confidence of the found solutions and can help to detect potential supercell solutions.

Following successful indexing, the pattern was treated using Jana2006 [12], and a sequence of Le Bail fitting without symmetry assumptions (in space group *P*1), preliminary space group assignment, and Le Bail fitting in the assigned symmetry was performed. The structure solution was performed via the Superflip routine [13] with subsequent Rietveld refinement both within Jana2006 (Table 2, Figure 2). Given the limitations of powder X-ray diffraction in the accurate refinement of lighter atom parameters, the displacement ellipsoids were modeled isotropically. The isotropic displacement parameters for N1 and N2 (the crystallographically inequivalent nitrogen atoms in the ammonia molecules) were constrained to equal values, as were those of O21 and O22 (bridging oxygen atoms within one of the two inequivalent nitrate groups). The hydrogen atoms of the ammonia molecules were modelled as riding on the nitrogen atoms, and their U_{iso} was constrained to be 1.2 times the U_{iso} of the N atoms (as suggested by Jana2006).

Table 2. Refinement details for $Ni(NH_3)_2(NO_3)_2$.

Chemical Formula	**$Ni(NH_3)_2(NO_3)_2$**
Formula Weight	216.8
Crystal system	Orthorhombic
Spacegroup	$Pca2_1$ (No. 29)
a/Å	11.0628(5)
b/Å	6.0454(3)
c/Å	9.3526(4)
V/Å^3	625.49(5)
Z	4
crystallographic density/g cm^{-3}	2.31(5)
No of data, parameters	4120, 68
R_p; wR_p	0.044, 0.060
R_{obs}; wR_2(all)	0.033, 0.044

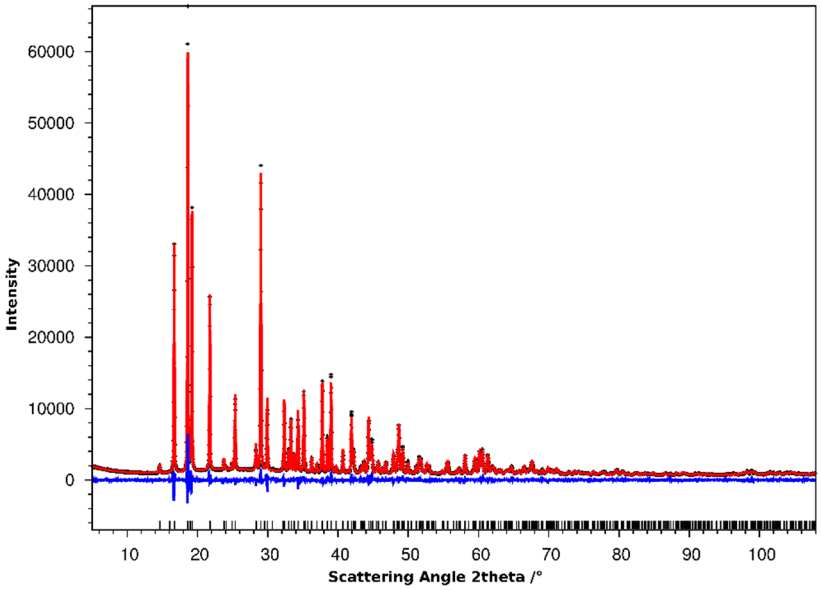

Figure 2. Plot of the measured powder pattern (black crosses) and calculated pattern (red line). The difference plot, (I_{obs}—I_{calc}), is denoted by the blue line and the theoretical peak positions are shown as black ticks.

2.3. Crystal Structure of $Ni(NH_3)_2(NO_3)_2$

$Ni(NH_3)_2(NO_3)_2$ crystallises in the orthorhombic, non-centrosymmetric space group $Pca2_1$ (a = 11.0628(5) Å, b = 6.0454(3) Å, c = 9.3526(4) Å, V = 625.49(5) Å^3) with eleven non-hydrogen atoms in the asymmetric unit (Figure 3). The structure consists of a three-dimensional network of compressed $[Ni(NH_3)_2(NO_3)_4]$ octahedra connected through four bridging nitrate anions per metal centre (and hence, each individual nitrate ligand bridges two metal centres, Figure 4). The nitrate ligands are located in the equatorial positions with the ammonia ligands trans- to one-another in the axial positions. This structure type presents the first evidence of bridging nitrate ligands in octahedral ammine complexes. In fact, the only other crystal structures of ammine complexes containing nitrates as ligands are the copper nitrate di- and monoammines [14] and platinum diammine dinitrate [15], where the nitrate and ammonia ligands are coordinated to the metal centres in a square planar geometry. Unlike these copper and platinum compounds, which achieve three-dimensional connectivity through hydrogen bonds, $Ni(NH_3)_2(NO_3)_2$ is connected in all three dimensions via bridging nitrate anions.

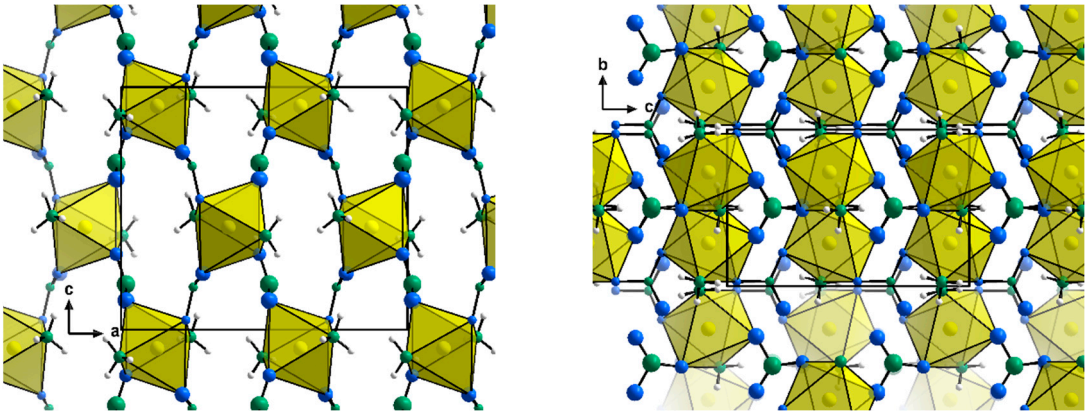

Figure 3. Representation of a unit cell of $Ni(NH_3)_2(NO_3)_2$ along (**a**) the crystallographic *b*-direction and (**b**) the crystallographic *a*-direction. Ni (gold), N (green), and O (blue) atoms are represented by their displacement spheres at 90% probability, while H (white) atoms are given as generic balls.

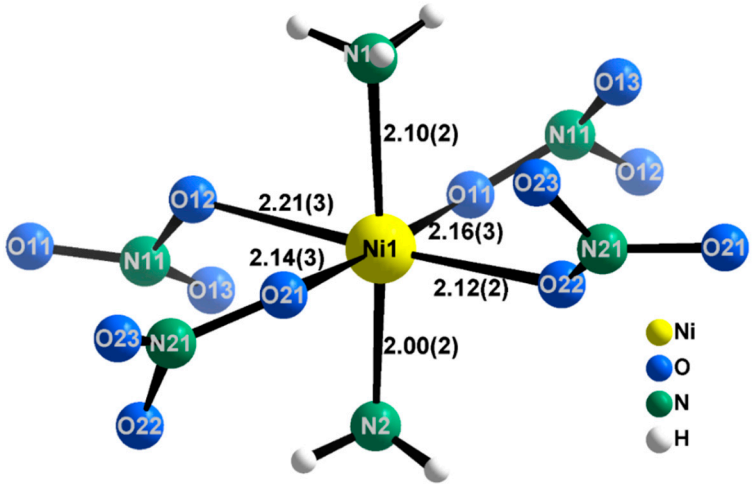

Figure 4. Coordination sphere around the nickel centre (Ni1) in the crystal structure of $Ni(NH_3)_2(NO_3)_2$. The Ni–ligand distances are given in Å. Ni (gold), N (green), and O (blue) atoms are represented by their displacement spheres at 90% probability, while H (white) atoms are given as generic balls.

As expected from the presence of two different ligands in the first coordination sphere, the $[Ni(NH_3)_2(NO_3)_{4/2}]$ octahedra are not regular (Figure 4, Table 3). The two Ni–N bonds are shorter (2.00(2) Å and 2.10(2) Å) than the equivalent Ni–O bonds (2.12(2) Å–2.22(3) Å) and the angles deviate slightly from the ideal octahedral values, resulting in compressed octahedra along the axial direction. Further, the N–O distances in the nitrate anion are also strongly anisotropic and range from 1.16(6) Å–1.32(6) Å. It is likely that the differences in the nitrate bond lengths are caused by comparatively strong hydrogen bonding interactions between the ammonia ligands and the terminal oxygen atoms in the nitrate anions (eight N–H···O hydrogen bonds with H···O $\leq$ 2.57 Å). The nitrate anion itself is also distorted in the plane of the nitrogen and oxygen atoms, departing from an ideal trigonal planar (D_{3h}) geometry with out-of-plane torsion angles <(O11–O12–O13–N11) = $-12(5)^\circ$ and <(O21–O22–O23–N21) = $-14(4)^\circ$. It should be noted that the relatively large errors on the values of these torsion angles suggest that the crystallographic evidence for the breaking of the D_{3h} nitrate anion symmetry is not in itself incontrovertible. Breaking of the symmetry, be it through the torsion of the molecule or the bonding of oxygen atoms, is however sensitive to detection by IR spectroscopy.

Table 3. Interatomic distances in $Ni(NH_3)_2(NO_3)_2$.

Atom 1	Atom 2	Distance/Å
Nitrate bonds		
N11	O11	1.23(6)
N11	O12	1.31(6)
N11	O13	1.16(6)
N21	O21	1.32(6)
N21	O22	1.25(4)
N21	O23	1.23(4)
Nickel–ligand bonds		
Ni1	N1	2.10(2)
Ni1	N2	2.00(2)
Ni1	O11	2.16(3)
Ni1	O12	2.21(3)
Ni1	O21	2.14(3)
Ni1	O22	2.12(2)

2.4. IR Spectroscopy of $Ni(NH_3)_2(NO_3)_2$

The ammonia vibrational modes in diammine nickel nitrate are very similar to those in diammine nickel chloride and hexammine nickel nitrate (Figure 5, Table 4). A notable exception, however, is that the symmetric deformation band, δ_s(HNH), in hexammine nickel nitrate is split for the diammine compounds. This can be understood in terms of the more pronounced hydrogen bonding in the diammine complexes as compared to hexammine nickel nitrate. This is consistent with the symmetry inequivalence of the two ammonia ligands in $Ni(NH_3)_2(NO_3)_2$ and hence supports the crystallographic model (where the two ammonia nitrogen positions are inequivalent).

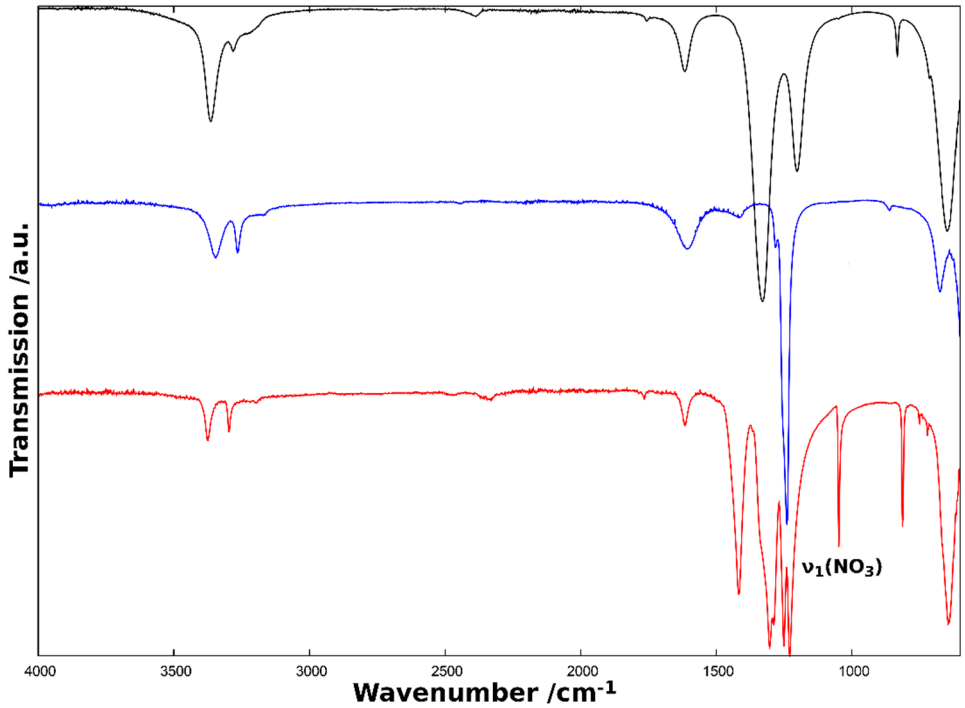

Figure 5. FTIR spectrum of $Ni(NH_3)_2(NO_3)_2$ (red) in comparison with the spectra of $Ni(NH_3)_2Cl_2$ [4] given in blue and $Ni(NH_3)_6(NO_3)_2$ [5] given in black.

Inclusion of nitrate anions within the first coordination sphere leads to an inevitable lowering of the molecular symmetry compared to the free nitrate anion [16] and hence leads to the appearance of further bands in the infrared spectrum [17]. Regarding the nitrate anion modes, several supplementary IR bands are observed in diammine nickel nitrate as compared to the equivalent hexammine (Figure 5). This can be attributed to the different bonding environments of the species. While the nitrate anion in hexammine nickel nitrate is not coordinated directly to the complex and therefore exists with ideal D_{3h} molecular symmetry, the same is not true for diammine nickel nitrate. The supplementary bands can be explained most clearly by comparison to the IR spectrum of the ethylenediamine (en) complex, $Ni(en)_2(NO_3)_2$ [17]. Most significantly, the appearance of the symmetric stretching mode (ν_1) at 1048 cm^{-1} is a clear and unambiguous indicator of the breaking of the ideal D_{3h} symmetry of the NO_3^- anion. Whereas this mode is inactive for a trigonal species of D_{3h} symmetry (since the dipole moment does not change), it becomes active when the three-fold rotation axis is lost (resulting in either C_{2v} or C_s symmetry). This occurs when the ligand is coordinated to a metal and the three nitrate oxygen atoms are no longer equivalent. Two further vibration modes that are degenerate for D_{3h} symmetry, the asymmetric stretching mode (ν_3) and the in-plane bending mode (ν_4), lose their degeneracy and are observed as separate bands in the IR spectrum of $Ni(NH_3)_2(NO_3)_2$. Furthermore, two sets of combination modes ($\nu_1 + \nu_3$ and $\nu_1 + \nu_4$) appear with the aforementioned fundamental modes and the supplementary out-of-plane mode ν_2.

Table 4. Assignment of the infrared bands in $Ni(NH_3)_2(NO_3)_2$ in comparison to the documented values of $Ni(en)_2(NO_3)_2$ (en = ethylenediamine) [17], $Ni(NH_3)_2Cl_2$ [4], and $Ni(NH_3)_6(NO_3)_2$ [5].

Band	**Wavenumber/cm^{-1}**			
	$Ni(NH_3)_2(NO_3)_2$	**$Ni(en)_2(NO_3)_2$ [17]**	**$Ni(NH_3)_2Cl_2$ [4]**	**$Ni(NH_3)_6(NO_3)_2$ [5]**
$\nu_a(NH_3)$	3375	-	3346	3364
$\nu_s(NH_3)$	3296	-	3265	3282
$2\delta_a(HNH)$	3195	-	3167	3167
$\nu_1 + \nu_3(NO_3)$	2475	2455	-	-
$\nu_1 + \nu_3(NO_3)$	2330	2320	-	-
$\nu_1 + \nu_4(NO_3)$	1765	1762, 1741	-	-
$\delta_a(HNH)$	1616	-	1607	1616
$\nu_3(NO_3)$	1417	1420	-	1329
$\nu_3(NO_3)$	1303	1303	-	
$\delta_s(HNH)$	1250	-	1281	-
$\delta_s(HNH)$	1229	-	1239	1202
$\nu_1(NO_3)$	1048	1033, 1034	-	-
$\nu_2(NO_3)$	812	818	-	823
$\nu_4(NO_3)$	751	728	-	-
$\nu_4(NO_3)$	721	708	-	-
$\rho(NH_3)$	643	-	675	648

3. Materials and Methods

3.1. Synthesis

$Ni(H_2O)_6(NO_3)_2$ (99%, BDH Chemicals, Poole, Dorset, UK) was used as supplied. The title compound was synthesised through the thermal decomposition of $Ni(NH_3)_6(NO_3)_2$, made from $Ni(H_2O)_6(NO_3)_2$ as described previously [5]. $Ni(NH_3)_6(NO_3)_2$ was heated under mild dynamic vacuum (*ca.* 10^{-2} bar) to 100 °C for 30 min in order to remove any remaining humidity from the compound. The complex was then further heated to 200 °C for 2 h under the same conditions to decompose the hexammine into the diammine. The completeness of the reaction could be followed by observing the change of the compound colour from purple to green.

3.2. Thermal Analysis

Thermal analyses were conducted on a Netzsch 409 PC STA instrument under flowing argon gas (99.998%, BOC, Guildford, Surrey, UK) coupled to a Hiden Analytical HPR 20 mass spectrometer. Combined TG–DTA–MS studies were conducted at a heating rate of 5 K min^{-1}. The STA instrument was located inside an argon-filled glove box (UNIlab, MBraun, Garching, Germany) with O_2 and H_2O levels below 3 ppm to avoid possible reactions of the samples with moist air. The samples were loaded into Al_2O_3 sample holders.

3.3. Fourier Transform Infrared (FTIR) Spectroscopy

Infrared spectra were collected on an attenuated total reflection Fourier-transform infrared (ATR-FTIR) spectrometer (FTIR-8400S; Shimadzu, Tokyo, Japan) over a range between 4000–600 cm^{-1}. A total of 24 accumulated spectra were collected with a resolution of 2 cm^{-1}.

3.4. Powder X-ray Diffraction

Samples of the hexammine and diammine were loaded into glass capillaries (Hilgenberg, 0.7 mm diameter) and flame-sealed. Samples was measured in Debye–Scherrer geometry on a Bruker D8 Advance diffractometer (Bruker AXS, Billerica, MA, USA) with Cu-Kα_1 radiation ($5^\circ \leq 2\theta \leq 108^\circ$, step size = 0.025°). Powder data were analysed as discussed in Section 2.2. These data can be obtained free of charge via www.ccdc.cam.ac.uk/conts/retrieving.html or deposit@ccdc.ca.ac.uk).

4. Conclusions

From an investigation of the thermal decomposition of $Ni(NH_3)_6(NO_3)_2$ it was possible to determine the synthetic conditions required to isolate the diammine nickel nitrate, $Ni(NH_3)_2(NO_3)_2$. Subsequent synthesis enabled the phase-pure polycrystalline diammine to be obtained and the structure solution to be performed from powder X-ray diffraction data. $Ni(NH_3)_2(NO_3)_2$ crystallises in the orthorhombic space group $Pca2_1$ and forms a novel structure type in which Ni centres are octahedrally coordinated by ammonia and nitrate in axial and equatorial positions, respectively. The latter ligands bridge to form a three-dimensional network. Using vibrational spectroscopy, we could both substantiate the chemical inequivalence of the two trans-ammonia ligands and confirm the involvement of the nitrate groups as ligands via signature bands attributable to the breaking of the ideal D_{3h} trigonal planar symmetry. Following similar strategies should facilitate the isolation and characterisation of further metal nitrate ammines and clarify the reaction pathways involved in deammoniation.

Supplementary Materials: The following are available online at http://www.mdpi.com/2304-6740/6/2/59/s1: cif-file for $Ni(NH_3)_2(NO_3)_2$ (CCDC- 1847082).

Author Contributions: J.B. and D.H.G. conceived and designed the experiments; J.B. performed the experiments and analysed the data; J.B., A.G.-J. and D.H.G. authored the paper. A.G.-J. and D.H.G. supervised the research.

Acknowledgments: D.H.G. thanks Airbus Group Innovations for funding a studentship for J.B.

Conflicts of Interest: The authors declare no conflict of interest.

References

1. Zamfirescu, C.; Dincer, I. Using ammonia as sustainable fuel. *J. Power Sources* **2008**, *185*, 459–465. [CrossRef]
2. Sørensen, R.Z.; Hummelshøj, J.S.; Klerke, A.; Reves, J.B.; Vegge, T.; Nørskov, J.K.; Christensen, C.H. Indirect, Reversible High-Density Hydrogen Storage in Compact Metal Ammine Salts. *J. Am. Chem. Soc.* **2008**, *130*, 8660–8668. [CrossRef] [PubMed]

3. Reardon, H.; Hanlon, J.M.; Grant, M.; Fullbrook, I.; Gregory, D.H. Ammonia Uptake and Release in the MnX_2–NH_3 (X = Cl, Br) Systems and Structure of the $Mn(NH_3)_nX_2$ (n = 6, 2) Ammines. *Crystals* **2012**, *2*, 193–212. [CrossRef]
4. Breternitz, J.; Vilk, Y.E.; Giraud, E.; Reardon, H.; Hoang, T.K.A.; Godula-Jopek, A.; Gregory, D.H. Facile Uptake and Release of Ammonia by Nickel Halide Ammines. *ChemSusChem* **2016**, *9*, 312–321. [CrossRef] [PubMed]
5. Breternitz, J.; Farrugia, L.J.; Godula-Jopek, A.; Saremi-Yaramahdi, S.; Malka, I.E.; Hoang, T.K.A.; Gregory, D.H. Reaction of $[Ni(H_2O)_6](NO_3)_2$ with gaseous NH_3; crystal growth *via* in-situ solvation. *J. Cryst. Growth* **2015**, *412*, 1–6. [CrossRef]
6. Migdał-Mikuli, A.; Mikuli, E.; Dziembaj, R.; Majda, D.; Hetmańczyk, Ł. Thermal decomposition of $[Mg(NH_3)_6](NO_3)_2$, $[Ni(NH_3)_6](NO_3)_2$ and $[Ni(ND_3)_6](NO_3)_2$. *Thermochim. Acta* **2004**, *419*, 223–229. [CrossRef]
7. Mikuli, E.; Migdał-Mikuli, A.; Majda, D. Thermal decomposition of polycrystalline $[Ni(NH_3)_6](NO_3)_2$. *J. Therm. Anal. Calorim.* **2013**, *112*, 1191–1198. [CrossRef]
8. Visser, J.W. A fully automatic program for finding the unit cell from powder data. *J. Appl. Crystallogr.* **1969**, *2*, 89–95. [CrossRef]
9. Werner, P.-E.; Eriksson, L.; Westdahl, M. TREOR, a semi-exhaustive trial-and-error powder indexing program for all symmetries. *J. Appl. Crystallogr.* **1985**, *18*, 367–370. [CrossRef]
10. Boultif, A.; Louër, D. Indexing of powder diffraction patterns for low-symmetry lattices by the successive dichotomy method. *J. Appl. Crystallogr.* **1991**, *24*, 987–993. [CrossRef]
11. Le Bail, A. Monte carlo indexing with mcmaille. *Powder Diffr.* **2004**, *19*, 249–254. [CrossRef]
12. Petříček, V.; Dušek, M.; Palatinus, L. Crystallographic Computing System JANA2006: General features. *Z. Kristallogr. Cryst. Mater.* **2014**, *229*, 345–352. [CrossRef]
13. Palatinus, L.; Chapuis, G. SUPERFLIP—A computer program for the solution of crystal structures by charge flipping in arbitrary dimensions. *J. Appl. Crystallogr.* **2007**, *40*, 786–790. [CrossRef]
14. Morozov, I.V.; Korenev, Y.M.; Troyanov, S.I. Synthesis and crystal structure of New Amminecopper(II) Nitrates: $[Cu(NH_3)_2](NO_3)_2$ and $[Cu(NH_3)](NO_3)_2$. *Z. Anorg. Allgem. Chem.* **1996**, *622*, 2003–2007. [CrossRef]
15. Lippert, B.; Lock, C.; Rosenberg, B.; Zvagulis, M. *cis*-Dinitratodiammineplatinum(II), *cis*-$Pt(NH_3)_2(NO_3)_2$. Crystalline structure and vibrational spectra. *Inorg. Chem.* **1977**, *16*, 1525–1529. [CrossRef]
16. Addison, C.C.; Logan, N.; Wallwork, S.C.; Garner, C.D. Structural aspects of co-ordinated nitrate groups. *Q. Rev. Chem. Soc.* **1971**, *25*, 289–322. [CrossRef]
17. Curtis, N.F.; Curtis, Y.M. Some Nitrato–Amine Nickel(II) Compounds with Monodentate and Bidentate Nitrate Ions. *Inorg. Chem.* **1965**, *4*, 804–809. [CrossRef]